Medical Science

25(117), November, 2021

Anatomical radiographic evaluation of vidian canal and its surrounding structures using Cone-beam computed tomography (CBCT)

Nasim Shams[1], **Mahshid Razavi**[1], **Saeid Shirafkan**[1], **Maryam Mohebinia**[2]✉

To Cite:
Shams N, Razavi M, Shirafkan S, Mohebinia M. Anatomical radiographic evaluation of vidian canal and its surrounding structures using Cone-beam computed tomography (CBCT). Medical Science, 2021, 25(117), 2842-2849

Author Affiliation:
[1]Assistant Professor, Department of Oral and Maxillofacial Radiology, Faculty of Dentistry, Ahvaz Jundishapur University of Medical Sciences, Ahvaz, Iran
[2]Resident of Oral and Maxillofacial Radiology, Department of Oral and Maxillofacial Radiology, Faculty of Dentistry, Ahvaz Jundishapur University of Medical Sciences, Ahvaz, Iran

✉**Corresponding author**
Resident of Oral and Maxillofacial Radiology, Department of Oral and Maxillofacial Radiology,
Faculty of Dentistry, Ahvaz Jundishapur University of Medical Sciences, Ahvaz, Iran

Peer-Review History
Received: 24 September 2021
Reviewed & Revised: 26/September/2021 to 30/October/2021
Accepted: 31 October 2021
Published: November 2021

Peer-review Method
External peer-review was done through double-blind method.

ABSTRACT

Background: Vidian canal (VC) is a vital surgical landmark in endoscopic endonasal skull base surgery. The aim of the present study was to evaluate the Vidian canal location and its anatomic surrounding using CBCT. *Materials and methods*: This study was a retrospective, cross-sectional research conducted on CBCT images of 100 patients from 2020 to 2021. The images were analyzed on the coronal and axial plane as follows: the length of VC, the VC-VC distance, VC-foramen rotundum (FR) distances, VC pterygopalatine plate (MPP) distance, pattern of VC pneumatization into the sphenoid sinus, location of the VC relative to the medial MPP, the angle of the VC and the palatovaginal canal, and the angle between the posterior of the middle turbinate and the lateral part of the VC. *Results*: The mean distance of VC-VC was 21.42 ± 3.27mm. The mean distance of VC on the right and left side was 14.43 ± 3.42 and 14.60 ± 3.12mm, respectively. The position of VC relative to MPP was 39.5% medially, 53.5% on the same line, and 11.5% laterally. The pattern of pneumatization showed 24.5% of patients was in grade I pneumatization, 40.5% grade II, 32.5% grade III, and 2.5% grade IV. *Conclusion:* Preoperative radiographic of skull base is paramount to appropriate surgical procedures. Precise determination of VC and its relationships with surrounding landmarks can reduce the surgical risks and improves the success rates of surgical procedures.

Keywords: Vidian canal; CBCT, palatovaginal canal, pterygoid canal

1. INTRODUCTION

The eponyms Vidian artery, Vidian canal, Vidian nerve, and Vidian vein, are derived first by Italian surgeon and anatomist Guido Guidi (Latin: VidusVidius) (Bahşi, 2020). The pterygoid canal or Vidian canal (VC) is the osseous tunnel in skull base which allows the Vidian artery and Vidian nerve pass through the pterygopalatine fossa to the middle cranial fossa. Vidian

DISCOVERY SCIENTIFIC SOCIETY
© 2021 Discovery Scientific Society. This work is licensed under a Creative Commons Attribution 4.0 International License.

© 2021 Discovery Scientific Society. All Rights Reserved. ISSN 2321–7359 EISSN 2321–7367 I OPEN ACCESS

nerve is formed in the area of the foramen lacerum with superficial and deep petrosal nerves and moves in the pterygoid canal transmitting the parasympathetic fibers. Sympathetic nerve fibers largely regulate nasal mucosa and parasympathetic nerve fibers control and regulate the gingival crevicular fluid, mucous secretions from the oral cavity and nasal cavity (Bahşi et al., 2019). Vidian canal, also known as VC, is the main indicator of internal carotid artery (Kurt et al., 2020).

Surgical endoscopic endonasal approach (EEA) is an advanced, safe and effective surgical technique with a low complication rate used to treat skull base lesions and also control the symptoms of vasomotor rhinitis through Vidianneurectomy (Kasemsiri et al., 2013; Prevedello et al., 2010). Endoscopic sinus surgery requires exact and detailed knowledge of anatomic variations in paranasal sinus region (Yeğin et al., 2017). Morphometric analysis and localization of Vidian canal (VC) and its connections with surrounding anatomical structures are necessary for successful management of endoscopic sinus surgery and Vidian neurectomy (Bahşi et al., 2019). As a full and complicated area with different passages, the skull base allows the spinal cord, blood vessels, and nerves all pass through. So, clinical assessment of skull base diseases is often difficult or incomplete. Imaging technique before and after skull base surgery is a good guidance for management of skull base diseases. Computed tomography (CT) is the gold standard method for morphological and morphometric analysis of skull base anatomy (Yazar et al., 2007).

CBCT (cone-beam computed tomography) is a volumetric medical diagnostic imagingmodality with accurate, high resolution, and three-dimensional (3D) volumetric data that allows the anatomic study of dental and maxillofacial bone structures. CBCT provides accurate images with high resolution (less than. 0.1 mm) and lower radiation doses than conventional CT scans (Bahşi et al., 2019). Some radiological and anatomical researches have been designed for better comprehension of anatomical variables and corresponding distances between landmarks using the anatomical landmarks of skull base area. Localization and position of the VC and adjacent anatomical structures increases the success of surgery and reduces possible complications. The aim of the present study was to determine the position of VC and its surrounding structures using cone-beam computed tomography (CBCT).

2. MATERIALS AND METHODS

Study design

The present retrospective cross-sectional study was conducted on the CBCT images of 100 patients (50 men and 50 women, age range: 18 to 80 years) retrieved from the archives of the Department of Oral and Maxillofacial Radiology, Faculty of Dentistry, Ahvaz Jundishapur University of Medical Sciences from 2020 to 2021. A total of 200 Vidian canals were evaluated. Inclusion criteria included patients over 18 years of age who had no history of facial surgery, trauma, nasal polyps, and sinonasal trauma.

CBCT images preparation

CBCT images were obtained using New Tom VGi CBCT imaging unit (QR SRL Co., Verona, Italy) with 110 kV peak exposure time, 2.04 mAh, time of 3.6 seconds and 12×8-inch fov. The CBCT images were processed using NNT Viewer software (QR SRL, Verona, Italy) and reconstructed to be viewed in coronal, sagittal, and axial plan. All measurements were made in a dimly lit room by a resident of radiology and confirmed by a maxillofacial radiologist with five years of experience. Images were displayed on a 16-inch Samsung monitor (Samsung Co, Korea, 1366 x 768 Pixel Resolution, 5ms Response Time).

CBCT evaluation

The images in coronal and axial plane were reconstructed at voxel size of 0.4 mm3 and a slice thickness and interval of 1 mm. The following morphometric parameters were measured on the coronal plane: the VC-VC, VC-MPP (medial pterygopalatine plate), and VC-FR (foramen rotundum) distances (Figure 1).

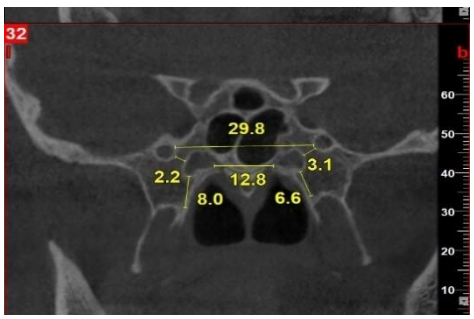

Figure 1 Distances between Vidian canal and surrounding structures on the coronal plane

© 2021 Discovery Scientific Society. All Rights Reserved. ISSN 2321–7359 EISSN 2321–7367 I OPEN ACCESS

The pattern of the VC pneumatization (relative to the sphenoid sinus) on coronal plane was measured as follows: Grade I: entirely surrounded by bone; Grade II: VC environed by air for 33% of the circumference; Grade III: VC environed by air for 33–66% of the circumference; Grade IV: VC almost entirely environed by air) (Vescan et al., 2007) (Figure 2). The VC location into to the MPP recorded as either medial, lateral, and on the same line (Type A: the VC located medially to the medial pterygopalatine plate, Type B: the VC located on the same line to medial pterygopalatine plate, Type C: VC waslocated laterally to medial pterygopalatine plate (Bahşi et al., 2019) (Figure 3).

The angle between the end of the posterior middle turbinate and theplace of the VC anterior opening and the angle between palatovaginal canal and VC were measured on axial plane. Similarly, the length of VC and the depth of pterygopalatine fossa (PPF) were measured on the axial plane, accordingly (Figure 4).

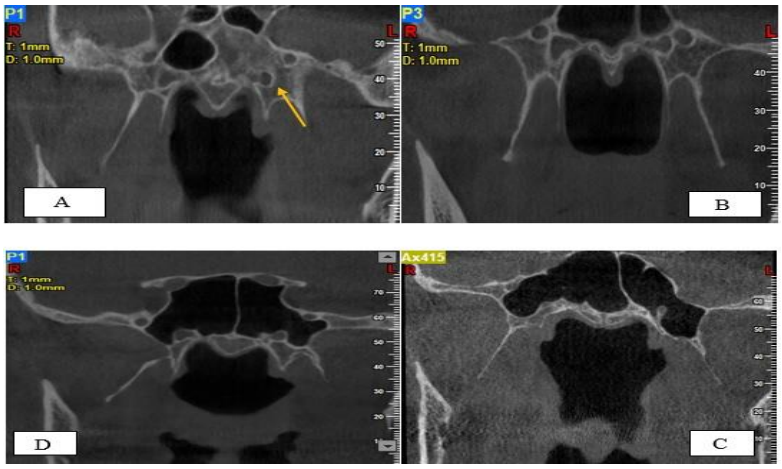

Figure 2 The pattern of the VCpneumatization (relative to the sphenoid sinus) on the coronal plane

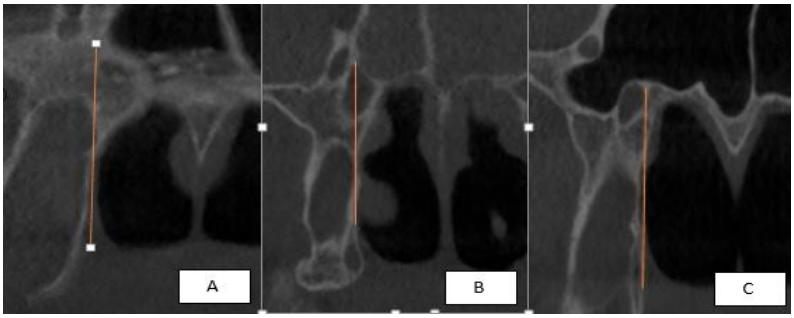

Figure 3 location of VC in medial pterygopalatine plate in the coronal plane: (A: medial; B: on the same line; C: lateral)

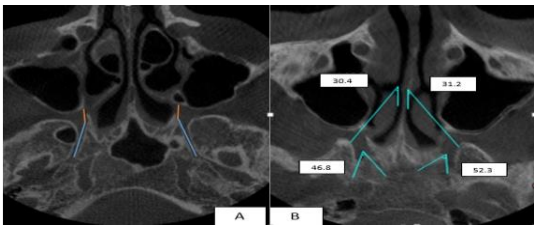

Figure 4 The VC measurement on the axial plane

Statistical analysis

In the present study, descriptive statistics were used to describe/summarize the characteristics of data set such as a variable's mean and standard deviation. The paired sample t-tests were conducted to define whether the mean differences between sides and genders were significant ($p \leq 0.05$). One-way analysis of variance (one-way ANOVA) was used to compare means of two or more samples (p-value≤0.05). Data were analyzed using SPSS version 23 (SPSS Inc., Chicago, IL, USA).

© 2021 Discovery Scientific Society. All Rights Reserved. ISSN 2321–7359 EISSN 2321–7367 I OPEN ACCESS

3. RESULTS

A total of 200 images of Vidian canal of 100 patients (male=50, mean age: 41.4; female=50, mean age: 44.4) were analyzed. Table 1 and 2 measure VC and its surroundings in two planes of coronal and axial are presented in Table 1 and 2.

Table 1 Descriptive statistics and the results of the measurements by gender in the coronal and axial plane (p<0.05)

	Total	male	Female	p-value
VC-VC (mm)	21.42±3.27272	21.8340±3.00670	21.0060±3.49999	.207 > 0.05
VC-FR (mm)	4.5155±1.67327	4.3270±1.67320	4.7040±1.66874	.262 > 0.05
VC-MPP (mm)	7.723±1.67568	7.7640±1.64543	7.6820±1.72111	.808 > 0.05
Length VC (mm)	14.5465±3.00724	15.0490±2.86902	14.0540±3.08604	.100 > 0.05
PPF depth(mm)	5.704±102061	5.7870±0.98700	5.6210±1.05657	.419 > 0.05
Angle between palatosphenoid canal and VC	51.0205±7.59083	52.5680±9.10881	49.4730±5.34411	.041 < 0.05
Angle between the end of the posterior middle turbinate and the place of VCanterior opening	33.893±10.81093	32.7630±9.69899	35.0230±11.80938	.298 > 0.05

Table 2 Descriptive statistics and the results of the measurements by side in the coronal and axial plane (p < 0.05)

	Total	right	left	p-value
VC.FR (mm)	4.5155±1.67327	4.462±1.9375	4.569±1.70955	0.679 > 0.05
VC.MPP (mm)	7.723±1.67568	7.517±1.86721	7.929±1.71984	0.106 > 0.05
lenght.VC(mm)	14.5465±3.00724	14.4313±3.4252	14.607±3.12417	0.706 > 0.05
PPF Depth(mm)	5.704±1.02061	5.716±1.08644	5.692±1.18045	0.881 > 0.05
Angle between palatosphenoid canal and VC	51.0205±7.59083	51.584±7.8771	50.457±9.01727	0.348 > 0.05
Angle between the end of the posterior middle turbinate and the place of VCanterior opening	33.893±10.81093	33.602±12.33001	34.184±10.66476	0.721 > 0.05

The morphometric parameters on the coronal plane: the VC-VC, VC-MPP, and VC-FR distances and the morphometric parameters on the axial plane (The VC length, PPF depth, the angle between the end of the posterior middle turbinate and lateral portion of the anterior opening VC, and the angle between VC and palatosphenoidal canal) in men were more than women. A significant difference was found in the angle between the palatosphenoidal canal and the VC in men than women. No significant difference was found between other variables. The angle between lateral part of VC anterior opening and end of the posterior middle turbinate in women was more than men, which was not statistically significant. There were no differences between right and left VC measurement (p>0.05).

In this study, mean length of VC was 14.54±3.0 (right side=14.43±3.42, left side= 14.60±3.12) and the measurements did not differ significantly by side (p>0.05). Additionally, the location of the VC into the MPP was evaluated. The results showed that in 39.5% of cases the VC was positioned medially, 53.5% was laid on the same line, and in 7% of cases it was positioned laterally. The mean VC-VC distances when the VC locates lateraly into the MPP were significantly high in the right side than medial and same line position. As well as, the mean VC-FR distances when the VC locates medial to the MPP were higher in the right side than the same line position. When VC location was lateral and medial to MPP, VC-MPP distance was significantly greater on the left side; however, it was greater on the medial position (p≤0.05) (Table 3).

The degree of pneumatization relative to the circumference of VC (into the sphenoid sinus) was evaluated. The results showed that 24.5% of the patients were grade I, 40.5% were grade II, 32.5% were grade III, and 2.5% were grade IV. VC-FR distance on the right side was significantly greater in images which exhibited grade III pneumatization compared to Grade I andII pneumatization. TheVC-VC and VC-MPP distances on the right side did not differ in images exhibiting grade I, II, III, and IV pneumatization. The VC-VC distance on the left side was significantly longer in images exhibiting grade I compared to Grade II pneumatization. The VC-FR distance on the left side similar to right side was significantly longer in images exhibiting grade III pneumatization compared to Grade I and II pneumatization (all p≤0.05) (Table 4).

© 2021 Discovery Scientific Society. All Rights Reserved. ISSN 2321–7359 EISSN 2321–7367 I OPEN ACCESS

Table 3 Comparison of the parameters of the VC's position relative to MPP (ANOVA) ($p < 0.05$)

	Side	Location VC Relative to MPP	Medial	Straight	Lateral
VC-VC	Right	Medial	21.2462±3.56543	0.297	0.007
		Straight	0.297	21.6273±2.85692	0.037
		Lateral	0.007	0.037	25.30±2.37065
	Left	Medial	21.2462±3.5411	0.987	0.088
		Straight	0.987	21.1404±3.11097	0.064
		Lateral	0.088	0.064	23.7889±2.07753
VC-MPP	Right	Medial	7.9875±2.00872	0.087	0.898
		Straight	0.087	7.1673±1.73547	0.870
		Lateral	0.898	0.870	7.6000±1.54434
	Left	Medial	8.4026±1.80824	0.163	0.047
		Straight	0.163	7.7500±1.59966	0.363
		Lateral	0.047	0.363	6.9111±1.51364
VC -FR	Right	Medial	5.0575±2.05886	0.038	0.418
		Straight	0.038	4.0782±1.81666	0.983
		Lateral	0.418	0.983	3.92±1.03779
	Left	Medial	5.000±1.85174	0.086	0.836
		Straight	0.086	4.2327±1.66754	0.778
		Lateral	0.836	0.778	4.6444±0.71083

Table 4 Comparison the distance of VC-VC, VC-MPP, and-FR and VC-VC according to pneumatization grades (ANOVA)

		Pneumatization degree	Grade 1	Grade 2	Grade 3	Grade 4
VC-VC	Right	Grade 1	21.413±2.58691	0.994	0.994	0.995
		Grade 2	0.994	21.1932±3.35125	0.936	0.917
		Grade 3	0.994	.936	21.6533±3.81112	0.977
		Grade 4	0.955	0.917		22.4667±.95044
	Left	Grade 1	22.5±3.42485	0.045	0.731	0.974
		Grade 2	0.045	20.3324±3.23128	0.304	0.522
		Grade 3	0.731	0.304	21.6486±2.99140	0.855
		Grade 4	0.974	0.522	0.855	23.5±1.55563
VC-MPP	Right	Grade 1	7.4478±1.68250	0.998	1.000	0.858
		Grade 2	0.998	7.5341±1.98716	0.998	0.881
		Grade 3	1.000	0.998	7.46±1.72459	0.858
		Grade 4	0.858	0.881	0.858	8.3667±3.49619
	Left	Grade 1	8.1077±1.76293	0.833	0.999	0.907
		Grade 2	0.833	7.7324±1.72708	0.873	0.981
		Grade 3	0.999	0.873	8.0429±1.74647	0.923
		Grade 4	0.907	0.981	0.923	7.25±.63640
VC-FR	Right	Grade 1	3.8435±1.54856	1.000	0.001	0.532
		Grade 2	1.000	3.8545±1.53129	0.000	0.514
		Grade 3	0.001	0.000	3.92±1.03779	0.957
		Grade 4	0.532	0.514	0.957	4.0782±1.81666
	Left	Grade 1	3.4885±1.53631	0.197	0.000	0.953
		Grade 2	0.197	4.2351±1.37259	0.000	0.998
		Grade 3	0.000	0.000	5.7433±2.17932	0.381
		Grade 4	0.953	0.998	0.381	5.3±1.40000

© 2021 Discovery Scientific Society. All Rights Reserved. ISSN 2321–7359 EISSN 2321–7367 I OPEN ACCESS

4. DISCUSSION

Vidian canal (VC) is a vital surgical landmark in surgical (EEA) for treatment of lesions of skull base and nonallergic rhinitis (vasomotor rhinitis) (Kasemsiri et al., 2013; Prevedello et al., 2010). When the sphenoid sinus is fully pneumatized, its relationship to the surrounding structures becomes very close, and the surrounding arteries and nerves are seen in the irregularities or ridges of the sinus cavity. When the sinus is extensively pneumatized, the relations of the sinus into the surrounding structures become very close and the surrounding vessels and nerves are realized in the sinus cavity as irregularities or ridges. The sphenoid pneumatization to the pterygoid processes is an extension of the sinus between the maxillary and Vidian nerves (Bahşi, 2020). The present study used CBCT imaging technique for measurement of the VC and its relationships with surrounding anatomic structures.

Mato et al., (2014) examined the anatomical features of VC and its relationships between VC and surrounding key landmarks using computed tomography (CT) scans and concluded that VC is a determining factor for the extent of bone drilling throughout surgery. The mean length of VC in the Mato et al.'s (2014) study was 14.4mm on the right side and 14.7mm on the left side. In this study the VC length was 14.43 (right side) and 14.60 (left side). The VC length in the similar previous studies was reported from 10 to 19mm. Kassam et al., (2005) suggested that VC-FR (foramen rotundum) distance was determinant for surgical endoscopic endonasal approach. This study showed that VC-FR distance was 4.46±1.93 on the left and 4.56±1.70 on the right side. The VC-FR distance in the similar previous studies was reported from 4 to 8.5mm (Kasemsiri et al., 2013; Yeh & Wu, 2013; Bryant et al., 2014).

In this study, the mean ± SD of VC-VC in coronal plane was evaluated (21.42±0.64) and no significant gender difference was found in the mean VC-VC distance. The extent of pneumatization is a vital guide for the surgeon throughout endoscopic endonasal surgery. If pneumatization pattern is marked actually, less bone drilling and removal is required throughout the exposure of the operative region. Moreover, the probability of a specified surgical injury to surrounding anatomical structures, such as the FR or anterior ethmoidal "genu" of the internal carotid artery will be reduced (Kurt et al., 2020). The degree to which VC pneumatized into the sphenoid sinus differs by VC type. This study preferred the following classification for grading pneumatization by VC circumference due its simplicity and accuracy: Grade I: entirely surrounded by bone; Grade II: VC environed by air for 33% of the circumference; Grade III: VC environed by air for 33–66% of the circumference; Grade IV: VC almost entirely environed by air (Vescan et al., 2007).

Kurt et al., (2019) reported grade II VCs in 33% of cases, and grade IV VCs in 19.5% of cases. Acar et al., (2019) reported Grade I VCs in 55.6 of cases, Grade II in 34.8% of cases, and Grade III in 9.6% of cases. Bolger et al., (2005) highlighted that Grade III VC was associated with a high risk of damage to contiguous structures. Vescan et al., (2007) suggested that the mean distance of VC-FR was larger when grade III or IV pneumatization was apparent on the either right or left side, which consistent with the results of Kurt et al.'s study (2020). Therefore, preoperative CT evaluation provides useful information for preoperative surgical planning. VC is a bony tunnel which connects between middle cranial fossa and pterygopalatine fossa. Various variations are associated with the direction, configuration, and length of VC. During EEA, the medial pterygoid plate (MPP) is frequently drilled along the inferior medial border of VC, so determination of the position of VC relative to the MPP during planning surgery is necessary (Vescan et al., 2007). In this study, the location of the VC into the MPP was evaluated. In 39.5% of cases the VC was positioned medially, 53.5% was located on the same line, and in 7% of cases it was sited laterally. Yeh and Wu, (2013) in a study showed that the location of the VC into the MPP was positioned medially or straight (98.1%), and in 1.9% of cases the VC was positioned laterally. Kurt et al., (2019) found that the VC was laid medially to the MPP in 54.5% of cases, 36% on the same line, and 9.5% was laid laterally. Yazar et al., (2019) and Bahşi et al., (2007) suggested that VC position to MPP was frequently found on the same line. The differences in VC position in the related studies could be explained due to racial disparities and differences in the demographic characteristics.

This study reported that mean distance of VC-VC on the right side was significantly larger when the VC was positioned laterally to MPP. Furthermore, the mean distance of VC-MPP on the left side was significantly larger when the VC was positioned medially to MPP ($p \leq 0.05$) (Table 3). Kurt et al., (2019) found that the mean distances of VC-FR and VC-VC on the right side were significantly larger, when the VC was positioned laterally to the MPP and the mean distance of VC-MPP on the left side was significantly larger, when the VC was positioned laterally to the MPP. During EEA, it is required to expose pterygopalatine fossa in order to access the anterior opening of VC. Thus, it is necessary to determine the precise depth of the pterygopalatine fossa. In this study, the mean pterygopalatine fossa depth was 5.71 ± 1.08 (right side) and 5.69 ± 1.18 mm (left side). The wider dimensions of the pterygopalatine fossa have been reported in various studies (6.7 to 7.1 mm on both sides). The reason could be explained due to differences in the study populations (Japanese, Caucasian, and Turkish) (Kurt et al., 2020; Vescan et al., 2007; Tsutsumi et al., 2018).

© 2021 Discovery Scientific Society. All Rights Reserved. ISSN 2321–7359 EISSN 2321–7367 I OPEN ACCESS

Since a scarce noticeable or hypertrophic turbinate may affect success rate of EEA, the measurement of the angle between the end of the posterior middle turbinate and the place of VC anterior opening is a prerequisite to surgical planning. In this study, this angle was 33.60 ± 12.33°on the right and 34.18 ± 10.66° on the left sideand no significant difference was found on the left and right sides. Acar et al., (2019) reported the mean angle of 33.05 ± 7.71. Kurt et al., (2019) reported the mean angles of 34.94 ± 9.93 (right side) and 32.07 ± 8.2° (left side), which indicated the greater angle on the right side than the left side. The palatovaginal canal (pharyngeal canal) is an intraoperative landmark for determination of VC. Thus, good basic radiological anatomy knowledge is essential to avoid delusional identification of the palatovaginal canal rather than VC (Karligkiotis et al., 2014). This study reported that the angles between palatovaginal canal and VC were 51.58 ± 7.87 on the left and 50.45 ± 9.017° on the right side.

5. CONCLUSION

This study provides an overview of the VC position and its relationship to surrounding anatomical structures such as FR and MPP using CBCT. Due to anatomical and radiological variations of VC, preoperative radiographic analysis of skull base is recommended for selection of appropriate surgical procedures. The results obtained by this study can helpsurgeons get a better view of VC and its relationships with surrounding landmarks. This reduces the surgical risks and improves the success rates of surgical procedures. Further studies with other ethnic groups are recommended.

Acknowledgment

Authors would like to express sincere gratitude to Vice Chancellor for Research and Technology, Ahvaz Jundishapur University of Medical Sciences (AJUMS) for the technical and financial support for this study.

Ethical Statement

The study was approved by the Ethics Committee of AJUMS Registration No: IR.AJUMS.REC.1400.094.

Funding

This study has not received any external funding.

Conflict of Interest

The authors declare that there are no conflicts of interests.

Data and materials availability

All data associated with this study are presented in the paper.

REFERENCES AND NOTES

1. Açar G, Çiçekcibaşı AE, Çukurova İ, Özen KE, Şeker M, Güler İ. The anatomic analysis of the vidian canal and the surrounding structures concerning vidianneurectomy using computed tomography scans. Braz J Otorhinolaryngol 2019; 85:136-43.
2. Bahşi I, Orhan M, Kervancıoğlu P, Yalçın ED, Aktan AM. Anatomical evaluation of nasopalatine canal on cone beam computed tomography images. Folia morphol 2019; 78:153-162.
3. Bahşi İ, Orhan M, Kervancıoğlu P, Yalçın ED. Morphometric evaluation and clinical implications of the greater palatine foramen, greater palatine canal and pterygopalatine fossa on CBCT images and review of literature. Surg Radiol Anat 2019; 41:467-551.
4. Bahşi İ, Orhan M, Kervancıoğlu P, Yalçın ED. The anatomical and radiological evaluation of the Vidian canal on cone-beam computed tomography images. Eur Arch Otorhinolaryngol 2019; 276:1373-83.
5. Bahşi İ. Life of Guido Guidi (VidusVidius), who named the Vidian canal. Childs Nerv Syst 2020; 36:881-4.
6. Bolger WE. Endoscopic transpterygoid approach to the lateral sphenoid recess: surgical approach and clinical experience. Otolaryngol Head Neck Surg 2005; 133 20–26.
7. Bryant L, Goodmurphy CW, Han JK. Endoscopic and three-dimensional radiographic imaging of the pterygopalatine and infratemporal fossae: improving surgical landmarks. Ann Otol Rhinol Laryngol 2014; 123:111-6.
8. Karligkiotis A, Volpi L, Abbate V, Battaglia P, Meloni F, Turri-Zanoni M, Bignami M, Castelnuovo P. Palatovaginal (pharyngeal) artery: clinical implication and surgical experience. Eur Arch Otorhinolaryngol 2014; 271:2839-43.
9. Kasemsiri P, Solares CA, Carrau RL, Prosser JD, Prevedello DM, Otto BA, Old M, Kassam AB. Endoscopic endonasal

© 2021 Discovery Scientific Society. All Rights Reserved. ISSN 2321–7359 EISSN 2321–7367 I OPEN ACCESS

transpterygoid approaches: anatomical landmarks for planning the surgical corridor. Laryngoscope 2013; 123: 811-815.

10. Kassam AB, Gardner P, Snyderman C, Mintz A, Carrau R. Expanded endonasal approach: fully endoscopic, completely transnasal approach to the middle third of the clivus, petrous bone, middle cranial fossa, and infratemporal fossa. Neurosurg focus 2005; 19:1-0.
11. Kurt MH, Bozkurt P, Bilecenoğlu B, Kolsuz ME, Orhan K. Morphometric analysis of vidian canal and its relations with surrounding anatomic structures by using cone-beam computed tomography. Folia morphol 2020; 79:366-73.
12. Mato D, Yokota H, Hirono S, Martino J, Saeki N. The vidian canal: radiological features in Japanese population and clinical implications. Neurol Med Chir 2014: oa-2014.
13. Prevedello DM, Pinheiro-Neto CD, Fernandez-Miranda JC, Carrau RL, Snyderman CH, Gardner PA, Kassam AB. Vidian nerve transposition for endoscopic endonasal middle fossa approaches. Neurosurgery 2010; 67:478-484.
14. Tsutsumi S, Ono H, Ishii H, Yasumoto Y. Visualization of the vidian canal and nerve using magnetic resonance imaging. Surg Radiol Anat 2018; 40:1391-6.
15. Vescan AD, Snyderman CH, Carrau RL, Mintz A, Gardner P, Branstetter IV B, Kassam AB. Vidian canal: analysis and relationship to the internal carotid artery. Laryngoscope 2007; 117:1338-42.
16. Yazar F, Cankal F, Haholu A, Kiliç C, Tekdemir I. CT evaluation of the vidian canal localization. Clin Anat 2007; 20:751-4.
17. Yeğin Y, Çelik M, Altıntaş A, Şimşek BM, Olgun B, Kayhan FT. Vidian canal types and dehiscence of the bony roof of the canal: an anatomical study. Turk Arch Otorhinolaryngol 2017; 55:22-26.
18. Yeh I, Wu I. Computed tomography evaluation of the sphenoid sinus and the vidian canal. BENT 2013; 9:117–121.

© 2021 Discovery Scientific Society. All Rights Reserved. ISSN 2321–7359 EISSN 2321–7367 I OPEN ACCESS